COMPARISON STUDY OF CFD AND ARTIFICIAL NEURAL NETWORKS IN PREDICTING TEMPERATURE FIELDS INDUCED BY NATURAL CONVENTION IN A SQUARE ENCLOSURE

Shiyu ZHOU[1,*], Xiaoping LIU[2], Guangyue DU[2], Chuanze LIU[2], Yucheng ZHOU[2]

[*1] School of Thermal Engineering, Shandong Jianzhu University, Jinan 250101, Shandong, China

[2] School of Information and Electrical Engineering, Shandong Jianzhu University, Jinan 250101, Shandong, China

[*]Corresponding author; E-mail: zhou-1sy@163.com

Natural convection in an enclosure is a classical problem in heat transfer field. In this study, natural convection induced by the heat source in the enclosure is studied with two analysis methods, i.e. Computational Fluid Dynamics (CFD) and Artificial Neural Networks (ANN). The heat transfer in the enclosure is an unsteady process. During this process, the temperature fields in the enclosure are changing with time. The vertical temperature field of y=0 at one moment is picked up for investigation. Firstly, FLUENT software which is a simulation program of CFD is adopted to simulate the temperature fields under different computation conditions. Then part of the simulation condition's temperature data is picked for training an ANN model and the rest of data is used for validating the ANN model. It has been found from the comparison between the CFD simulation and ANN prediction that the two results have a good agreement with each other. In the comparison, the max relative errors (MAEs) are around 12 %, mean relative errors (MREs) are around 0.3 %, mean square errors (MSEs) are around 0.6 %, values of absolute fraction of variance (R^2) are all not less than 0.99. The results demonstrated that the ANN prediction have enough accuracy.

Key words*: Natural convection, CFD, Artificial neural network, Square enclosure.*

1. Introduction

The study about natural convective heat transfer in an enclosure has been conducted for several decades because of the classical properties of the problem [1,2]. Das, etal. [3] published a review about this scientific issue, they summarized the previous researches on natural convection heat transfer in an enclosure filled with fluid or porous media, including triangular, trapezoidal, parallelogrammic, or have an irregular shape with curved and wavy walls. Most of the studies about the natural convection in an enclosure with a heat source on the bottom were conducted numerically using the finite volume method and SIMPLER algorithm [4,5]. Minea [6] preferred numerical analysis in the investigation of the natural convection in a heated closed enclosure. They believed that natural convection in enclosed enclosures could be studied correctly only with numerical analysis. As an intelligent algorithm, artificial neural network (ANN) has been developed rapidly in recent years and applied in various studies [7]. This approach has also been applied in the heat transfer field, such as the prediction of temperature field [8]. The ANN's feasibility of predicting the thermal and flow variables due to natural convection in a complicated domain has been verified in several papers. The network prediction were usually validated with database generated by CFD software.

Mahmoud and Ben-Nakhi [9,10] employed three types of ANN to predict the heat transfer behavior in partitioned enclosures. They trained and tested the ANN architectures with the database obtained from CFD methodology. Their study demonstrated that ANN could effectively be used to predict the natural convection parameters with a significant reduction in the computation time and power. Varol et al. [11] predicted the natural convection thermal and flow variables in a triangular enclosure with ANN and Adaptive-Network-Based Fuzzy Inference System (ANFIS), respectively. By comparing with CFD computation results, they demonstrated that ANN and ANFIS were both capable of accurately predicting out the flow and thermal behavior within the enclosure. In their other study [12], they showed that the memory space and computation time could be significantly reduced by using ANFIS to accurately predict a buoyancy-induced flow field in a triangular enclosure. Sudhakar et al. [13] studied the mixed convection heat transfer within a 3D vertical duct with ANN in order to find out the optimum configuration for five discrete heat sources. In their study, the temperature database developed from CFD simulations was used to train the neural network and the trained ANN performed well in predicting the temperature of the heat source. Ozsunar [14] trained and tested a neural network with the results generated from a CFD program. The aim of the study was to find suitable parameters for a chip subjected to a constant heating power. The results obtained from the neural network model and the CFD program showed a good fit with a maximum error of 1.8%. Atayılmaz [15] applied a three-layers network in analyzing natural convection heat transfer in a horizontal cylinder. They compared the results from the trained network with the experimental Nusselt number over the cylinder and the results were in a good agreement.

In recent studies, applications of ANN or ANFIS in heat transfer field have been enriched and more complicated objects were studied. Selimefendigil and Oztop [16] employed a fuzzy based identification procedure to investigate the heat transfer process in a square cavity with an adiabatic fin. Karami et al. [17] reported the application of ANFIS in modelling the forced convection heat transfer from v-shaped plate internal surfaces exposed to an air impingement slot jet. They obtained an excellent consistency between the predicted and experimental results, which showed that ANFIS was a powerful flexible mathematical model. Yang et al. [18] developed an approach by combining the ANN and CFD to study the flow distribution in a quenching tank. The studied flow rate of the quenching medium showed a good agreement between the ANN prediction results and the CFD simulation data. In order to study the laminar natural convection in a square cavity, Aminossadati et al. [19] developed an ANFIS and an ANN approach, respectively. The developed approaches were trained and validated with the CFD analysis results. Their study showed that ANFIS and ANN could successfully predict the fluid flow and heat transfer behavior within the cavity. In the study of Taghavifar and Shabahangnia [20], the ANN was used to model a thermal process with four inputs and five outputs. Their study showed that the ANN was able to accurately predict temperature trend of airflow and plate. Ahamad and Balaji [21] developed an ANN to solve the inverse conjugate heat transfer problem, i.e. the heat source was predicted with trained temperature distribution by ANN. They validated the efficiency and accuracy of the ANN by comparing ANN predictions with experimental data. Ahmadi, et al. [22-25] have conducted a serious of researches relating with artificial neural networks. In their studies, ANN based on hybrid genetic algorithm and particle swarm optimization, GMDH (group method of data handling) neural networks, ANN-PSO (particle swarm optimization) and also ANN-ICA (imperialist competitive algorithm) were adopted to study the performance of stirling engine, and also to model the power and torque of stirling engine, and the results demonstrated the strong prediction ability of neural networks.

It can be inferred from the above analysis that plenty of research works have been done relating with ANN in heat transfer field. However, the purpose or significance of every references are different from each other. The purpose of this research is to study the heat storage and release property of different wood blocks by comparing temperature fields caused by a heated wood block with different initial temperatures. In this study, natural convection heat transfer in a square enclosure is studied using CFD and ANN, respectively. The results obtained from the two approaches are compared with each other. The paper is organized as follows. A physical model of the square enclosure with a wood block at the bottom middle is given in Section 2. Both CFD simulation and ANN prediction results are listed and compared in Section 3. The paper is concluded by Section 4.

2. Description of the study

2.1. Physical description

The studied enclosure in the paper is a cube whose physical structure is shown in Fig. 1. There is a square wood block located in the bottom middle of the enclosure. The parameters of the square enslosure and the wood block are shown in Tab. 1.

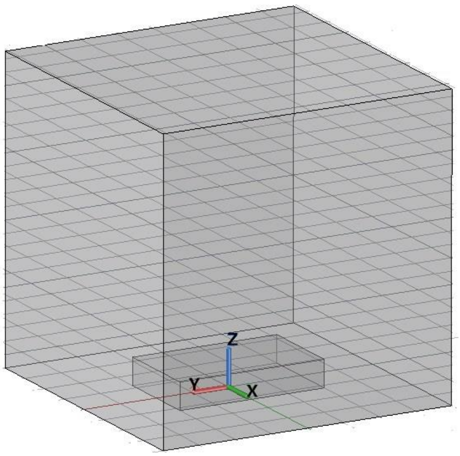

Fig. 1 Schematic diagram of the square enclosure

Tab. 1 Parameters of the studied object

	Square wall	**Block**	**Fluid**
Material property	Steel	Wood	Air
Size (mm)	L=W=H=200	L/W/H 100×60×18	
Density (kg/m^3)	8030	590	Boussinesq assumption
Thermal conductivity (W·m^{-1}K^{-1})	16. 27	0.1332	0.0259
Thermal capacity (J·kg^{-1}K^{-1})	502	1633	1005
Initial temperature (˚C)	T_a	T_0	T_a

Note: H-height, L-length, W-width;

2.2. Mathematical description

The following assumptions are adopted for simplification purpose.

1) Since the temperature differences of the studied conditions are not high (most less than 100˚C), Boussinesq assumption should be adopted for the approximation of air density [26].
2) The wood is actually porous medium. To simplify the simulation, however,the wood block is simplified as homogeneous and its thermal physical properties are kept constant in the simulation process.
3) The thermal contact resistances that between the wood block and the square wall are ignored.
4) The initial temperature of the steel wall, wood block and air are uniform.
5) The radiation heat transfer process is neglected.

The description of the flow and heat transfer in the square enclosed cavity with conservation equations of mass, momentum and energy are shown as following:

$$\frac{\partial u}{\partial x}+\frac{\partial v}{\partial y}+\frac{\partial w}{\partial z}=0 \tag{1}$$

$$\frac{\partial(\rho u)}{\partial t}+u\frac{\partial(\rho u)}{\partial x}+v\frac{\partial(\rho u)}{\partial y}+w\frac{\partial(\rho u)}{\partial z}=\frac{\partial}{\partial x}(\mu\frac{\partial u}{\partial x})+\frac{\partial}{\partial y}(\mu\frac{\partial u}{\partial y})+\frac{\partial}{\partial z}(\mu\frac{\partial u}{\partial z})-\frac{\partial P}{\partial x} \tag{2}$$

$$\frac{\partial(\rho v)}{\partial t}+u\frac{\partial(\rho v)}{\partial x}+v\frac{\partial(\rho v)}{\partial y}+w\frac{\partial(\rho v)}{\partial z}=\frac{\partial}{\partial x}(\mu\frac{\partial v}{\partial x})+\frac{\partial}{\partial y}(\mu\frac{\partial v}{\partial y})+\frac{\partial}{\partial z}(\mu\frac{\partial v}{\partial z})-\frac{\partial P}{\partial y} \tag{3}$$

$$\frac{\partial(\rho w)}{\partial t}+u\frac{\partial(\rho w)}{\partial x}+v\frac{\partial(\rho w)}{\partial y}+w\frac{\partial(\rho w)}{\partial z}=\frac{\partial}{\partial x}(\mu\frac{\partial w}{\partial x})+\frac{\partial}{\partial y}(\mu\frac{\partial w}{\partial y})+\frac{\partial}{\partial z}(\mu\frac{\partial w}{\partial z})-\frac{\partial P}{\partial z}+\rho g \tag{4}$$

$$\frac{\partial(\rho T)}{\partial t}+u\frac{\partial(\rho T)}{\partial x}+v\frac{\partial(\rho T)}{\partial y}+w\frac{\partial(\rho T)}{\partial z}=\frac{\lambda}{c}\left(\frac{\partial^2 T}{\partial x^2}+\frac{\partial^2 T}{\partial y^2}+\frac{\partial^2 T}{\partial z^2}\right) \tag{5}$$

In above equations, *u*, *v*, *w* are velocities in *x*, *y*, *z* directions, respectively; *t* is time; μ is viscosity of air; *P* is air pressure; *T* is air temperature; ρ is air density; *c* is air specific heat; *g* is acceleration of gravity. Energy equation in the wood block and square cavity wall is as follows:

$$\frac{\partial T}{\partial t}=\frac{\lambda}{\rho c}\left(\frac{\partial^2 T}{\partial x^2}+\frac{\partial^2 T}{\partial y^2}+\frac{\partial^2 T}{\partial z^2}\right) \tag{6}$$

In which, *T* is the temperature of the wood block or square wall; λ is the thermal conductivity of that; ρ is the density of that; while *c* is the specific heat of that.

3. Results and discussion

In this section, approaches of CFD and ANN are adopted to study the natural convection in the square enclosure. The data derived from CFD are picked for training and testing ANN. Although the studied enclosure is a 3-D model, only temperature field at one cross-section is studied for simplification. In this study, temperature field of the cross-section at y=0 is investigated. The heat transfer in the studied enclosure is an unsteady process, meaning that the temperature field is changing with time. To simplify the analysis, only temperature field at 9000 second is analyzed (the moment of 9000s after the heat exchange begins). In the ANN model, coordinates of *x* and *z*, together with the initial temperature of T_0, are defined as inputs; while temperature field at 9000s is defined as output. Computation conditions of initial temperatures (T_0) between 50-130˚C are studied, in which, the simulation data of T_0 = 50˚C /60˚C /70˚C/80˚C/90˚C/100˚C/110˚C/120˚C/130˚C are used for training the ANN model, while the simulation data of T_0 = 55˚C/65˚C/75˚C/85˚C /95˚C /105˚C/115˚C/125˚C are used for testing the trained ANN model.

3.1. CFD simulations

Computational Fluid Dynamics (CFD) is one of the most frequently used software packages for solving the heat transfer and flow problems because of its powerful numerical analysis and simulation ability. In which, FLUENT program is one of the most suitable simulation tool of CFD for this study. Therefore, FLUENT 6.3 is firstly adopted to simulate the heat transfer process in the square enclosure.

1) Boundary conditions (t = 0)

The initial temperatures of each medium are set as following:

Air temperature: T_a = 20 ˚C ;

Wood block: T_0 = 50˚C /55˚C /60˚C /65˚C……120˚C /125˚C /130 ˚C ;

Top surface: T_a = 20 ˚C ;

Side wall: T_a = 20 ˚C ;

Bottom surface: T_a = 20 ˚C ;

2) Check of grid independence

The computation results is usually affected by the mesh density. It is preferred to adopt as less number of grid as possible for accelerating the computation speed. However, it is only acceptable under the condition that the decrease of grid number has little effect on the accuracy of the computation results. In the simulation, five mesh generation schemes are conducted and compared, as shown in Tab. 2.

Tab. 2 Grid sizes and number of different mesh generation schemes

Scheme	Sc-1	Sc-2	Sc-3	Sc-4	Sc-5
Wood block	2mm	2mm	2mm	2mm	2mm
Fluid	2mm	2mm	3mm	3mm	5mm
Square wall	2mm	3mm	3mm	5mm	5mm
Grid number	1010230	888988	340921	277832	97659

In these schemes in Tab. 2, the hex grid is adopted for meshing the wood block and air, while the tet grid is adopted for meshing the square wall. In order to obtain the optimal meshing scheme, the temperature distributions along the center line of the studied enclosure under the five different schemes at the same moment (9000s) are compared, as shown in Fig. 2.

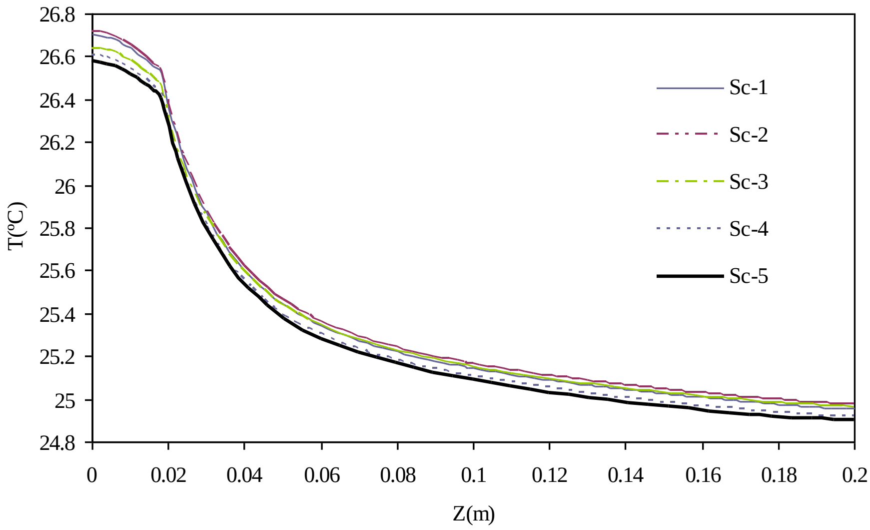

Fig. 2 Temperature curves of different meshing schemes (x=0, y=0)

It can be seen that, “Sc-2” is more closer to the “default accurate temperature” of “Sc-1” compared with other schemes. The average temperature difference between “Sc-1” and “Sc-2” is 0.0157˚C, which is acceptable for the simulation precision. Although the grid numbers of Sc-3, Sc-4 and Sc-5 are much less than Sc-1, the temperatures of the three schemes evidently deviate from the “default accurate temperature” of “Sc-1”. Therefore, the second grid division method (Sc-2) is employed for the following simulation works in this study.

3) Simulation and Validation

The simulation results of the two initial temperatures are selected for analysis, i.e. the computation conditions of T_0 = 50 ˚C and T_0 = 130 ˚C, as shown in Fig. 3.

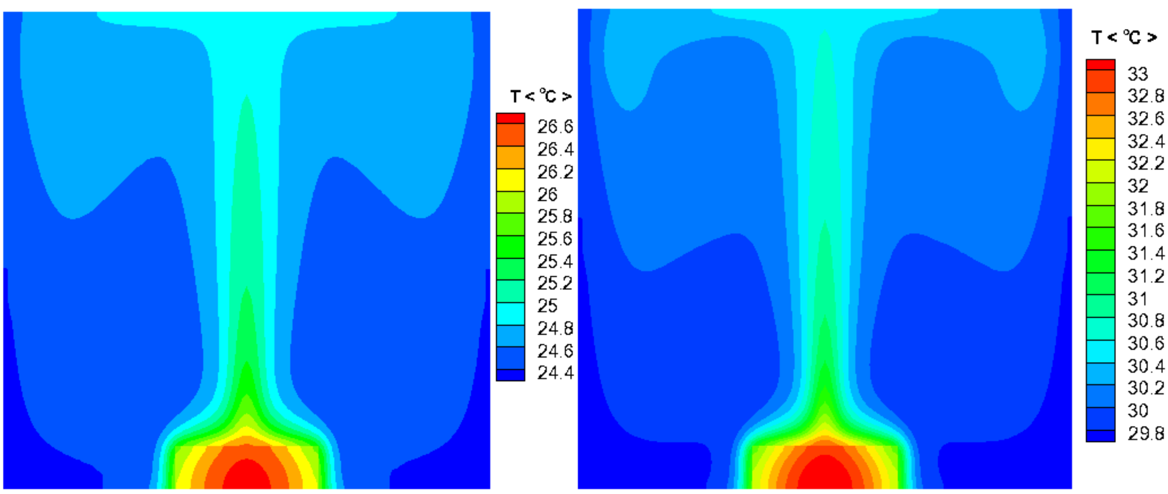

(a) T_0 = 50 ˚C (b) T_0 = 130 ˚C

Fig. 3 The results of CFD simulation at 9000s

It could be seen from the above figures that the temperature fields in the enclosure are symmetrical and ideal. Because the initial temperature of the wood block is much higher than the air temperature in the enclosure, the air surrounding the wood block is firstly heated, and then the heated air rises up for the reason of "chimney effect". At the same time, the unheated air converges at the two side-down corners for its lower temperature. As a result, the temperature fields induced by the nature convection are generated. It can also be concluded from the figures that the heat exchange is still in process at the moment of 9000s because of the existence of temperature difference. Besides, the highest temperature always emerges from the wood block since it is the heat source of the heat transfer in the square enclosure.

In order to validate the correctness of the CFD model, the same physical parameters together with the initial and boundary conditions as the research of Calcagni et al.[27] are set, and also be validated with their experimental results. The comparison results in Tab. 3 show that the CFD model in the present study has enough reliability.

Tab. 3 Comparison of *Nu* between this paper and study of Calcagni et al.[27]

Nu	$Ra=10^3$			$Ra=10^5$		
a	Calcagni etal.	Present study	Error /%	Calcagni etal.	Present study	Error /%
0.2	1.214	1.243	2.33	2.462	2.431	1.26
0.4	1.712	1.732	1.15	4.063	4.008	1.35

In the table, the following dimensionless parameters are adopted and compared:

$Ra = g\beta(T_0 - T_a)H^3 / \nu\alpha$, in which, g is acceleration of gravity; β is thermal expansivity; T_o is temperature of heat source; T_a is temperature of square wall; H is the height of enclosure; ν is dynamic viscosity; α is thermal diffusivity.

$Nu = -\partial T / \partial n$, in which, n is the normal direction of heat source surface (y=0). Nu_{ave} is the integral mean value of *Nu* along the heat source surface (y=0).

a=*w/W*, in which, *w* is the width of heat source, *W* is the width of square enclosure.

3.2. ANN predictions

Artificial neural network (ANN) offers a powerful tool for analyzing complicated problems without linear or other simple relations between input and output parameters. In this study, back propagation (BP) feed forward neural network is adopted for the temperature field prediction. Fig. 4 is the structure of the adopted ANN in this study. The hidden layer number or the number of neurons in each hidden layer could be confirmed by a neuron independence study. Too many neurons inevitably delay the convergence time and too few neurons could not give satisfactory performance.

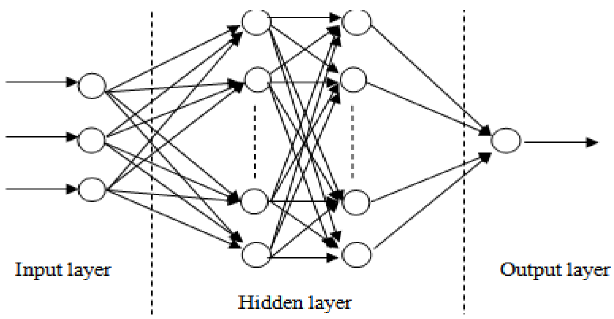

Fig. 4 Schematic diagram of ANN

1) BP neural network

BP neural network has become relatively mature both in network theory and in terms of performance. Fig. 5 is the frequently used model of BP neural. Its outstanding advantage is the strong nonlinear mapping ability and flexible network structure. The number of hidden layers and neurons in every hidden layers could be set according to the specific situation. And also, the BP network performance varies with the structure changing. Therefore, BP network is the most typical learning algorithm of multilayer neural network, and also it is good at local searching. However, there is also some inevitable problems existing in the network for its iterative steepest descent gradient algorithm. For example, different initial weights may lead to completely different results; the search process may end up with a local minimum; selection of relevant parameters such as learning rate and hidden layers largely depends on the experience and the network will not converge if the improper values are adopted [28].

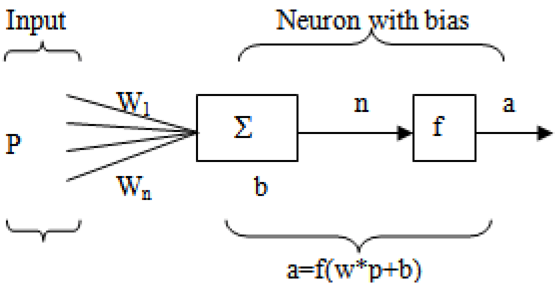

Fig. 5 Common model of BP neuron

2) Normalization and error computation

In order to improve the generalization ability of BP network, it is necessary to normalize the sample data into range of [-1,1] or [0,1] to ensure that all variables lie in the same scale, so as to eliminate the magnitude differences between different dimensional data and avoid big error induced by that. The normalization formulation of coordinates (*x*, *z*) and temperature *T* are as follows:

For coordinate *x* or *z*: $$\overline{x_i} = \frac{x_i - x_{mid}}{(x_{\max} - x_{\min})/2}, \text{ in which, } x_{mid} = \frac{x_{\max} + x_{\min}}{2} \tag{7}$$

For temperature *T*: $$\overline{T_i} = \frac{T_i - T_{\min}}{(T_{\max} - T_{\min})} \tag{8}$$

Transfer function which is also called activation function, i.e. Log-sig, tan-sig and also purelin functions are usually used in the BP network. In the AAN model, a linear function (purelin) is taken as the transfer function in the output layer of the BP model, while tan-sig function is adopted in the hidden layers. A neuron independence study has been conducted to determine the optimum network structure based on the following performance metrics: mean relative error (*MRE*) , max relative error (*MAE*), mean square error (*MSE*) and absolute fraction of variance (R^2). The above errors could be excellent criteria for evaluating the performance of the ANN network. A perfect fit could result in an R^2 value of 1 or a very good fit near 1. The fitting quality decreases as R^2 decreases.

$$MRE\ (\%) = \frac{1}{n}\sum_{i=1}^{n}\frac{|T_{ANN} - T_{CFD}|}{(T_{CFD-\max} - T_{CFD-\min})} \times 100 \tag{9}$$

$$MAE\ (\%) = Max(\frac{|T_{ANN} - T_{CFD}|}{T_{CFD-\max} - T_{CFD-\min}}) \times 100 \tag{10}$$

$$MSE\ (\%) = \sqrt{\frac{1}{n}\sum_{i=1}^{n}(T_{ANN} - T_{CFD})^2}\ /(T_{CFD-\max} - T_{CFD-\min}) \times 100 \tag{11}$$

$$R^2 = 1 - \frac{\sum_{i=1}^{n}(T_{ANN} - T_{CFD})^2}{\sum_{i=1}^{n}(T_{ANN} - T_{ANN-mean})^2} \tag{12}$$

3) Prediction results

Initial weights and biases have dominating effect on the prediction results. Therefore, it is important to choose proper weights and biases for the training of ANN. The conventional method for BP network to generate initial weights and biases is the *Nguyen-Widrow* method [29]. In this study, the training epoch is divided into several stages with equal number of epochs. In the first training stage, the initial weights and biases are generated with the *Nguyen-Widrow* method. When this training stage is over, the new weights and biases will be generated and used as the initial weights and biases for the second train stage, and so on. The prediction results demonstrate that this method has good reliability. The detailed information of the parameters adopted in the construction and also training of ANN are listed in Tab. 4.

Tab. 4 Parameters of ANN used in the study

Architecture	
The number of layers	3
The number of neuron on the layers	(15,15,1)
The initial weights and biases	The Nguyen-Widrow method
Activation functions	Tan-Sigmoid
Training parameters	
Learning rule	Back-propagation
Learning rate	0.005
Epoch	500
Momentum constant	0.9
Performance	3.62e-06

With the well trained network, the temperature fields of different computation conditions are predicted, and part of the results are shown in Fig. 6. In the figure, the left figures are the predicted results of ANN while the right figures are the simulated results of CFD. It can be seen that, the predicted temperature fields are not as ideal as the CFD simulations. But the temperature profiles of ANN and CFD at the same T_0 look almost the same as each other. For example, in the results of "T_0=55˚C" , the shape of the highest emperature area of ANN is evidently different from that of CFD, which just occupy a small propotion of the whole study area. In contrast, the lower temperature area especially the air distribution area of the two results, i.e. ANN and CFD are almost the same as each other, indicating that the two results match well enough. The difference between the two results of every computation conditions can be further illustrated with the computed errors that have been mentioned in the previous section, and the computed errors are shown in Tab. 5.

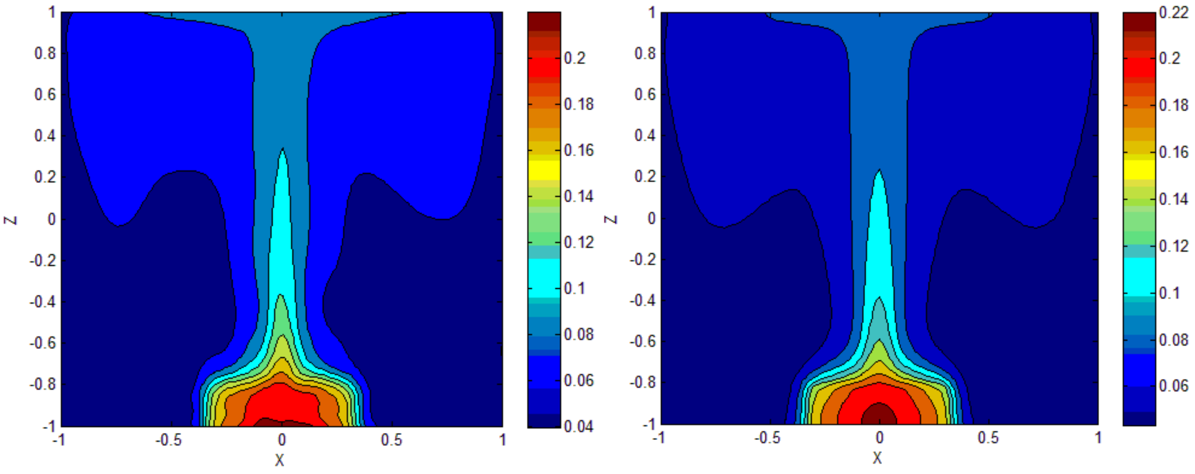

ANN CFD

(a) T_0=55˚C

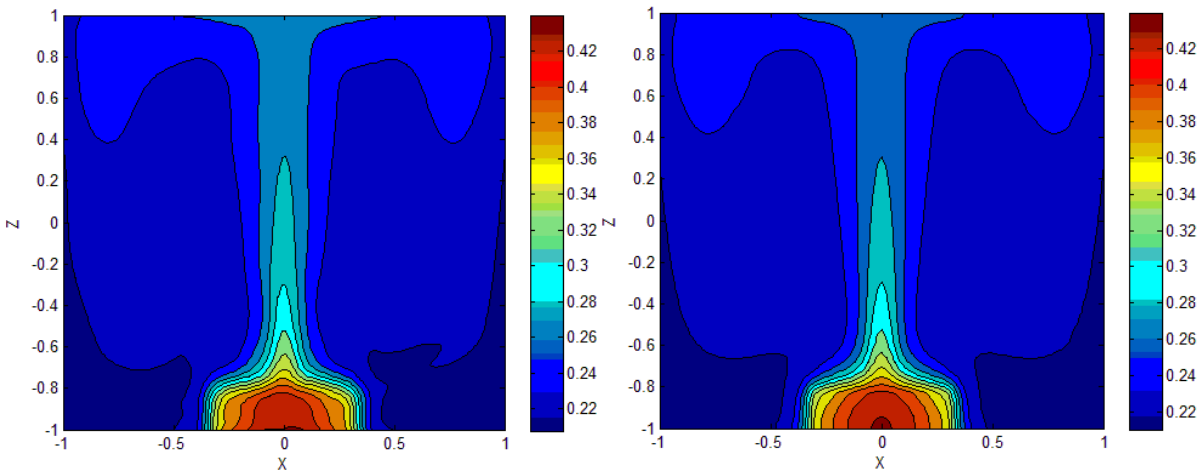

ANN CFD

(b) T_0=75 ˚C

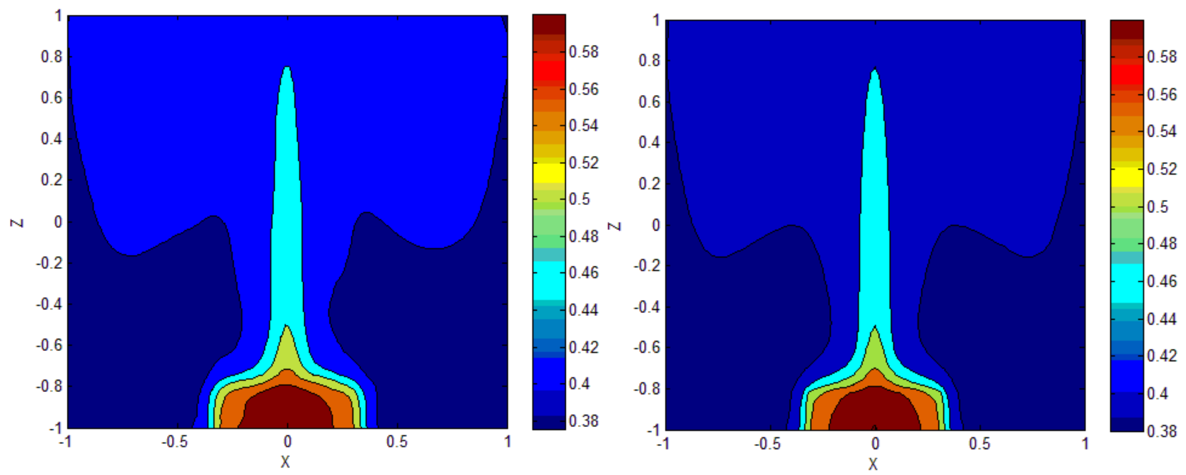

ANN CFD

(c) T_0=95˚C

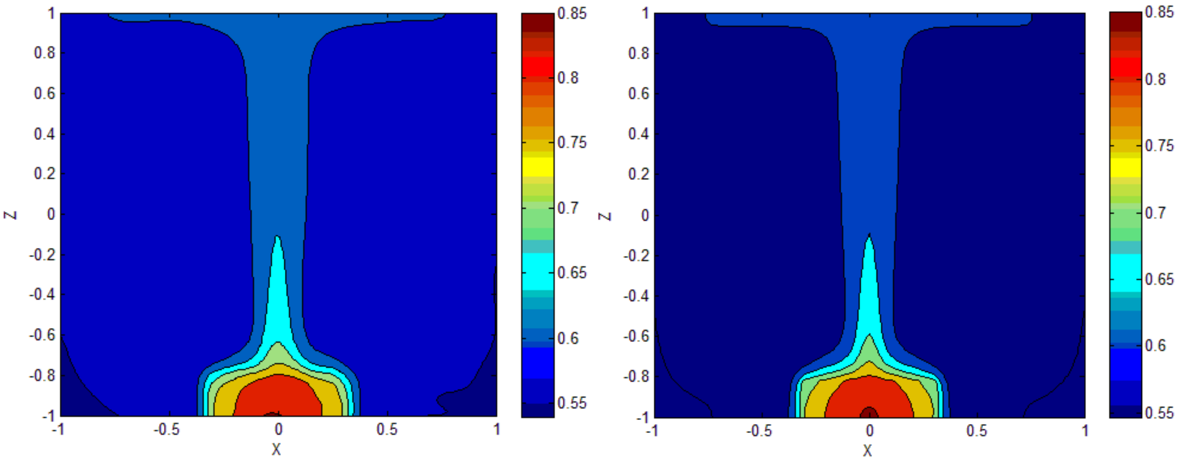

ANN CFD

(d) T_0=115˚C

Fig. 6 Comparison between ANN prediction and CFD simulation results

Tab. 5 Computed errors of temperature field at cross-section of y=0

T_0 (˚C)	*MRE* (%)	*MAE* (%)	*MSE* (%)	R^2
55	0.6218	13.0450	0.9311	0.9967
65	0.3797	13.0209	0.6950	0.9981
75	0.3498	12.9160	0.6630	0.9983
85	0.3104	12.8484	0.6416	0.9984
95	0.3184	12.7718	0.6434	0.9983
105	0.3181	12.9670	0.6452	0.9983
115	0.3278	11.6699	0.6455	0.9983
125	0.3547	13.7630	0.6916	0.9980

It can be seen from Tab.5 that the three computed errors for the eight predictions are all small enough, especially for *MRE* and *MSE*, which are all less than 1%, most of *MRE* values are around 0.3% while most of *MSE* values are around 0.6 %. There are inevitable several inaccurate predicted points for every predictions, leading to the relatively big value of *MAE*, which are around 12%. In general, these ANN predictions show good agreementS with the CFD simulation results, which can be illustrated by the high value of R^2 of every prediction. It can be concluded from the ablove anaylsis that the well trained ANN model can predict out temperature fields with enough accuracy.

4. Conclusions

The paper conducted a comparison study between the CFD simulation and ANN prediction on the analysis of the natural convection induced by a heat source in a square enclosure. The temperature field of a cross-section in the enclosure was choosen for comparison. For the comparison, a three layer ANN model was constructed and trained based on the part of database from CFD simulation, and the output of the well trained ANN model was validated according to the other part of CFD database. The validation was conducted from the mean relative error (*MRE*), max relative error (*MAE*), mean square error (*MSE*) and absolute fraction of variance (R^2). The small enough value of comparison errors and the R^2 value of closing to 1 demonstrated that, with the proper set of parameters in the construction and training of ANN model, good results could be predicted and that ANN was a reliable and convenient tool in the computation of temperature fields.

The current work is just a beginning of a series of study, 3-D research will be conducted in the future, and also the time factor in the unsteady process will be taken into consideration.

Acknowledgements

This work is financially sponsored by Taishan Scholar Project of Shandong Province of China.

Statements

On behalf of all authors, the corresponding author states that there is no conflict of interest.

References

[1] Lage, J. L., Bejan, A., The Ra-Pr domain of laminar natural convection in an enclosure heated from the side, *Numerical Heat Transfer Applications*, *Part A* 19 (1991), pp. 21-41

[2] Ntibarufata, E., *et al.*, Natural convection in partitioned enclosures with localized heating, *International Journal of Numerical Methods for Heat & Fluid Flow*, *3* (1993) , pp. 133-143

[3] Das, D., *et al.*, Studies on natural convection within enclosures of various (non-square) shapes – A review, *International Journal of Heat and Mass Transfer*, *106* (2017) , pp. 356-406

[4] Mahmoodi, M., *et al*., Free convection of a nanofluid in a square cavity with a heat source on the bottom wall and partially cooled from sides, *Thermal Science*, *18* (2014), (suppl.2) :283-300

[5] Jani, S., *et al*., Numerical investigation of natural convection heat transfer in a symmetrically cooled square cavity with a thin fin on its bottom wall, *Thermal Science*, *18*(2014),4, pp. 1119-1132

[6] Minea, A. A., A review on analytical techniques for natural convection investigation in a heated closed enclosure: Case study, *Thermal Science*, *19* (2015) ,3, pp. 1077-1095

[7] Oke. S. A., A literature review on artificial intelligence, *International Journal of Information and Management Sciences, 19* (2008) , pp. 535-570

[8] Erdemir, D., Ayata, T., Prediction of temperature decreasing on a green roof by using artificial neural network, *Applied Thermal Engineering*, *112* (2017) , pp. 1317-1325

[9] Mahmoud, M.A., Ben-Nakhi. A.E., Neural networks analysis of free laminar convection heat transfer in a partitioned enclosure, *Communications in Nonlinear Science and Numerical Simulation*, *12* (2007) , pp. 1265-1276

[10] Ben-Nakhi, A.E., *et al.*, Inter-model comparison of CFD and neural network analysis of natural convection heat transfer in a partitioned enclosure, *Applied Mathematical Modelling*, *32* (2008) , pp. 1834-1847

[11] Varol, Y., *et al.*, Prediction of flow fields and temperature distributions due to natural convection in a triangular enclosure using Adaptive-Network-Based Fuzzy Inference System (ANFIS) and Artificial Neural Network (ANN), *International Communications in Heat and Mass Transfer*, *34* (2007) , pp. 887-896

[12] Varol, Y., *et al.*, Analysis of adaptive-network-based fuzzy inference system (ANFIS) to estimate buoyancy-induced flow field in partially heated triangular enclosures, *Expert Systems with Applications*, *35* (2008) , pp. 1989-1997

[13] Sudhakar, T.V.V., *et al*., Optimal configuration of discrete heat sources in a vertical duct under conjugate mixed convection using artificial neural networks, *International Journal of Thermal Sciences*, *48* (2009) , pp. 881-890

[14] Ozsunar, A., *et al.*, The prediction of maximum temperature for single chips' cooling using artificial neural networks, *Heat & Mass Transfer*, *45* (2009) , pp. 443-450

[15] Atayılmaz, S.O., *et al.*, Application of artificial neural networks for prediction of natural convection from a heated horizontal cylinder, *International Communications in Heat and Mass Transfer, 37* (2010) , pp. 68-73
[16] Selimefendigil, F., Oztop, H.F., Fuzzy-based estimation of mixed convection heat transfer in a square cavity in the presence of an adiabatic inclined fin, *International Communications in Heat and Mass Transfer, 39* (2012) , pp. 1639-1646
[17] Karami, A., *et al.*, Adaptive neuro-fuzzy inference system (ANFIS) to predict the forced convection heat transfer from a v-shaped plate, *Heat & Mass Transfer*, *49*(2013), pp. 789-798
[18] Yang, X., *et al.*, Optimum design of flow distribution in quenching tank for heat treatment of A357 aluminum alloy large complicated thin-wall workpieces by CFD simulation and ANN approach, *Transactions of Nonferrous Metals Society of China*, *23*(2013) , pp. 1442-1451
[19] Aminossadati, S.M., *et al.*,Computational analysis of magnetohydrodynamic natural convection in a square cavity with a thin fin, *European Journal of Mechanics B/Fluids, 46* (2014) , pp. 154-163
[20] Taghavifar, H, Shabahangnia E., Prediction of thermal gradient in an air channel with presence of electrostatic field using artificial neural network, *Heat & Mass Transfer*, *50* (2014), pp. 1515-1524
[21] Ahamad, S. I., Balaji, C., Inverse conjugate mixed convection in a vertical substrate with protruding heat sources: a combined experimental and numerical study, *Heat & Mass Transfer , 52* (2016) , pp. 1243-1254
[22] Ahmadi, M. H., *et al*., Prediction of power in solar stirling heat engine by using neural network based on hybrid genetic algorithm and particle swarm optimization, *Neural Computing and Applications*, *22* (2013),6, pp. 1141-1150
[23] Ahmadi, M. H., *et al*., Using GMDH neural networks to model the power and torque of a stirling engine, *Sustainability*, *7* (2015), 2, pp. 2243-2255
[24] Ahmadi, M. H., *et al*., Artificial neural networks modelling of the performance parameters of the Stirling engine, *International Journal of Ambient Energy*, *37* (2016),4, pp. 341-347
[25] Toghyani, S., *et al*., Artificial neural network, ANN-PSO and ANN-ICA for modelling the Stirling engine, *International Journal of Ambient Energy ,37* (2016), 5, pp. 456-468
[26] Hamimid, S., *et al.*, Numerical study of natural convection in a square cavity under non-boussinesq conditions, *Thermal Science*, *20*(2016),5, pp. 1509-1517
[27] Calcagni, B., *et al*., Natural convective heat transfer in square enclosures heated from below, *Applied Thermal Engineering*, *25* (2005) , pp. 2522-2531
[28] Montana, D. J., Davis. L., Training feed-forward neutral networks using genetic algorithms, *Proceeding of the International Joint Conference on Artificial Intelligence*. Los Altos, 1989, pp. 762–767
[29] Liu, Q., *et al.*, Research on Initialization AIgorithms of Weights and Biases of BP Neural Netwok, *Jourml of Southwest Chim Nornlal University(Natural Science Edition) 35*(2010),6, pp. 137-141 (in chinese)